



HAL
open science

Ovarian cancer: An update on imaging in the era of radiomics

S. Nougaret, M. Tardieu, H.A. Vargas, C. Reinhold, S. Vande Perre, N. Bonanno, E. Sala, I. Thomassin-Naggara

► **To cite this version:**

S. Nougaret, M. Tardieu, H.A. Vargas, C. Reinhold, S. Vande Perre, et al.. Ovarian cancer: An update on imaging in the era of radiomics. *Diagnostic and Interventional Imaging*, 2018, 10.1016/j.diii.2018.11.007 . hal-02290882

HAL Id: hal-02290882

<https://hal.umontpellier.fr/hal-02290882v1>

Submitted on 20 Jul 2022

HAL is a multi-disciplinary open access archive for the deposit and dissemination of scientific research documents, whether they are published or not. The documents may come from teaching and research institutions in France or abroad, or from public or private research centers.

L'archive ouverte pluridisciplinaire **HAL**, est destinée au dépôt et à la diffusion de documents scientifiques de niveau recherche, publiés ou non, émanant des établissements d'enseignement et de recherche français ou étrangers, des laboratoires publics ou privés.



Distributed under a Creative Commons Attribution - NonCommercial 4.0 International License

Ovarian cancer: An update on imaging in the era of radiomics

S Nougaret¹ MD PhD, M Tardieu¹ PhD, HA Vargas² MD, C Reinhold³, S Van de Perre⁴, N Bonanno⁵ MD, E Sala⁶ MD PhD, I Thomassin-Naggara MD PhD⁴

1 Department of Radiology, IRCM, Montpellier Cancer Research Institute, INSERM, U1194, University of Montpellier, Montpellier 34295, France.

2 Department of Radiology, Memorial Sloan Kettering Cancer Center, New York, NY 10065, USA.

3 Department of Radiology, McGill University Health Center, Montreal, Canada

4 Department of Radiology, Hopital Tenon, Assistance Publique-Hôpitaux de Paris Sorbonne Universités - Institut des Sciences du Calcul et de Données (ISCD), 75020 Paris, France

5 Medical Imaging Department, Mater Dei Hospital, Malta

6 Department of Radiology, Box 218, Cambridge Biomedical Campus, Cambridge United Kingdom

Corresponding author: Stephanie Nougaret MD PhD

stephanienougaret@free.fr

Abstract

Tumor heterogeneity in ovarian cancer has been reported at the histological and genetic levels and are associated with adverse clinical outcomes. Tumor evaluation using standard computed tomography or magnetic resonance imaging techniques does not account for the intra- or inter-tumoral heterogeneity in advanced ovarian cancer with peritoneal carcinomatosis. As such, computational approaches in assessing tumor heterogeneity have been proposed using radiomics and radiogenomics in order to analyze the whole tumor heterogeneity as opposed to single biopsy sampling. As part of radiomics, texture analysis, which includes the extraction of multiple data from images has been proposed recently to evaluate advanced ovarian tumor heterogeneity. In this short review, we explain the basics of radiomics, how to perform texture analysis, and its applications to ovarian cancer imaging.

Index terms: Ovarian cancer; Radiomics; Texture analysis; Genomics; Advanced imaging

Introduction

Traditionally, radiologists subjectively evaluate clinical images based on their training and experience to provide a diagnosis or an assessment of a clinical state (e.g. treatment response evaluation). This approach introduces a high degree of variability in image interpretation. Tools for more automated imaging analyses have been tested, not only to reduce this variability, but to provide more objective clinically relevant information [1]. Furthermore, the role of computed tomography (CT) or that of magnetic resonance imaging (MRI) in cancer evaluation, especially in ovarian cancer is evolving. In the near future, a simple description of the tumor and its extent may not be sufficient when challenged regarding which molecularly-targeted drug to give or about early response to treatment and best timing for surgery [2, 3].

Radiomics has been introduced as an emergent tool for postprocessing CT or MR images and developing new quantification metrics linking qualitative and/or quantitative imaging data to clinical endpoints [4-10]. This may allow development of new biomarkers for diagnosis, prognosis and response evaluation [11, 12]. The term radiogenomics links imaging features with genomic data for the same purpose [13-17]. Initially, radiomics referred mainly to the extraction of multiple qualitative parameters assessed subjectively by a radiologist such as the presence of

tumor enhancement or tumor size [18]. In kidney cancer, for example, it was shown that mutations of VHL in clear cell type cancer were significantly associated with well-defined tumor margins, nodular tumor enhancement, and gross appearance of intra-tumoral vascularity at CT [18]. Recently, radiomics has embraced a more automated pathway with texture analysis (TA). TA is a form of radiomics which includes the extraction, analysis, and interpretation of quantitative features from medical images, leading to an exponential amount of data that can be correlated with tumor diagnosis, genomics and/or prognosis [19-31]. TA is of particular interest for the evaluation of tumor heterogeneity and has already demonstrated considerable potential in neuroradiology for lesion characterization [5, 32-34]. In renal cancer, TA has shown that features such as entropy and standard deviation were associated with histologic subtype and nuclear grade [35, 36]. Besides its correlation with histopathology, TA may also serve as a prognostic biomarker. In rectal cancer, T2-derived texture metrics extracted from the whole tumor volume have been shown to outperform the combination of T2- and diffusion-weighted images to assess complete response to therapy [37]. Ovarian cancer is a genomically diverse disease and such genomic and tumour microenvironment heterogeneity has been recently disease linked to platinum resistance [2]. Genomic evaluations performed by The Cancer Genome Atlas research group has shown large number of molecular alterations which may open new avenues to more targeted molecular based treatment [38-42]. The widespread disease associated with OC makes the evaluation of heterogeneity challenging both by single biopsy sampling and by traditional imaging tools. Therefore TA could be a potentially useful biomarker that allows assessment and quantification of tumor spatial heterogeneity and as such, better target the appropriate treatment in line with the tumor radiogenomic profile [3].

The purpose of this review is to describe how to perform TA, and discuss its current and potential applications in ovarian cancer imaging.

TA in ovarian cancer

Epidemiology

Ovarian cancer is the seventh diagnosed cancer among women in the world and epithelial type is the most predominant one [43, 44]. Ovarian cancer is subsequently divided into five major histopathology subtypes that differ in origin, pathogenesis, molecular alterations, risk factors,

and prognosis [45]. High-grade serous ovarian cancer (HGSOC), the focus of this review, is the most common histological subtype (representing 90% of ovarian cancers) with the least favorable prognosis [45]. Adjuvant or neoadjuvant treatment with platinum-based chemotherapy has response rates of 70–80 % but most patients have relapse and develop chemotherapy-resistant disease [46]. The five-year survival rate is less than 35% for patients with advanced ovarian cancer [46, 47]. As such, only marginal improvement in overall survival has been achieved over the past decades despite major medical advances. Recent data have shown that ovarian cancers have substantial molecular heterogeneity at presentation, which may explain drug resistance [2, 38-41, 48] Indeed, The Cancer Genome Atlas (TCGA) Research Network has performed copy number analysis, expression and methylation arrays, and exome sequencing of more than 18 500 genes in 489 cases of HGSOC [49, 50]. Nearly all tumors harbored a mutation in the p53 gene (TP53) as well as a large number of gene copy number alterations, which could explain this wide heterogeneity [50]. From this work, it was also found that *BRCA1/2* genes play a role in HGSOC, irrespective of germline status[51].

Additional work evaluating ovarian cancer heterogeneity at the genomic level has been done. Studies have shown that wide inter-tumoral heterogeneity exists at the genomic level between primary ovarian cancer and peritoneal implants [52-58]. Supporting these findings, a preliminary analysis of a small cohort of patients who underwent MRI examination has revealed that ovarian tumors and metastatic peritoneal implants are already phenotypically heterogeneous at the time of diagnosis [59]. In this study, including 22 patients, Sala et al. found significant differences in baseline apparent diffusion coefficient (ADC) values among primary ovarian cancer, omental cake and peritoneal deposits indicating for the first time that diffusivity profiles may be tumor-site dependent and suggesting the biologic heterogeneity of the disease for the first time on imaging[59].

Radiomics and radiogenomics:

Moving forward to the era of radiomics, radiogenomics analysis has been evaluated on ovarian cancer to correlate CT tumor phenotype with gene pattern and survival.

Qualitative analysis

Based on TCGA research network data, microarray-based transcriptomic profiles have been integrated as a prognostic algorithm for HGSOC known as classification of ovarian cancer (CLOVAR) [50]. Four prognostically relevant CLOVAR subtypes of HGSOC have been identified and labeled as: differentiated, immunoreactive, mesenchymal, and proliferative [60, 61]. Patients with mesenchymal subtype have a higher rate of platinum resistance (63%) compared with patients with other subtypes (23%), as well as shorter median survival (23 months for mesenchymal tumors vs. 46 months for other subtypes). Vargas et al. investigated the relationships between CT features and CLOVAR subtypes of HGSOC [62]. This study included 46 women with HGSOC, whose tumors were subjected to molecular analysis performed by TCGA [62]. Two readers independently evaluated multiple CT qualitative features of the primary ovarian tumor and sites of peritoneal carcinomatosis spread including location, shape, pattern of spread and implants size [62]. They found that CLOVAR mesenchymal subtype was significantly associated with higher risk of peritoneal involvement and the presence of mesenteric infiltration. In addition, they found that patients with HGSOC in whom mesenteric infiltration was identified on CT images had shorter progression-free survival and overall survival [62]. These results may explain the reported poorer prognosis of patients with the CLOVAR mesenchymal subtype of HGSOC [61]. More recently, those later results have been tentatively validated in a cohort of 92 patients with HGSOC with transcriptomic CLOVAR profiles [63]. Eight radiologists from the Cancer Genome Atlas Ovarian Cancer Imaging Research Group independently recorded multiples qualitative CT features. Similar associations were found between the extent of peritoneal involvement, time to progression, and CLOVAR subtypes. The presence of mesenteric infiltration as a poor prognostic factor in HGSOC was not validated in this study. One possible explanation is the poor interobserver agreement in the assessment of this feature ($\alpha = 0.23$) [63]. Indeed, this study highlight as well the low interobserver reproducibility of some imaging features and the limits of subjective evaluation which in turn advocates for the potential benefits of automated or semiautomated analysis [63].

Concomitantly to CLOVAR analysis, radiogenomics evaluation has been performed in the context of BRCA gene alterations. BRCA 1 and BRCA 2 play both a major role in DNA repair [64-67]. Several studies have suggested that patients with BRCA-mutant HGSOC have improved survival compared to those with BRCA wild-type HGSOC [68-78]. More favorable

prognosis of BRCA-mutant HGSOC has been linked to a greater sensitivity to platinum chemotherapy in primary and recurrent disease, as well as to unique tumor biology that confers survival advantage regardless of chemotherapy sensitivity [68, 71, 73-78]. In a study including 108 patients, Nougaret et al. evaluated multiple qualitative CT phenotypic tumor features that could explain the different behavior of these mutations [79]. These authors found that certain CT features of HGSOC differ based on the *BRCA* mutation status. Nodular peritoneal carcinomatosis implants pattern and presence of peritoneal disease in gastrohepatic ligament were associated with *BRCA*-mutant HGSOC at multiple regression analysis [79]. On the opposite, infiltrative peritoneal disease pattern, presence of mesenteric involvement, and supradiaphragmatic lymphadenopathy were associated *BRCA*-wildtype HGSOC. Those results are in line with histopathologic data that found peritoneal deposits with rounded or “pushing” contours associated with *BRCA*-mutant HGSOC, whereas *BRCA* wild-type HGSOC show infiltrative peritoneal implants [80-82]. It can be hypothesized that nodular type disease found in *BRCA* mutant HGSOC might achieve higher rate of complete cytoreductive surgery compared to infiltrative ill-defined disease found in *BRCA* wild-type HGSOC and this might explain the higher overall survival. However, statistical significance was not reached in Nougaret et al. study and larger cohort studies will be needed.

Quantitative analysis

As previously discussed, the subjective assessment of qualitative features may be limited by a poor interobserver reproducibility. In the study of Vargas et al., the interobserver agreement (between 8 readers) for the shape of the peritoneal disease (diffuse, no peritoneal disease, nodular, peritoneal enhancement only, predominantly diffuse, predominantly nodular) was only 0.353 [63]. As such, TA may decrease the variability of visual interpretation and may be of interest in the evaluation of ovarian cancer. In a study including 38 patients, Vargas et al. developed 12 quantitative metrics to capture spatial inter-site imaging heterogeneity in HGSOC [83]. The authors found that of the 12 inter-site texture heterogeneity metrics evaluated, those capturing the differences in texture similarities across sites were associated with shorter overall survival (inter-site similarity entropy, similarity level cluster shade, and inter-site similarity level cluster prominence; $P \leq 0.05$) and incomplete surgical resection (similarity level cluster shade, inter-site similarity level cluster prominence and inter-site cluster variance) [83]. On the

opposite, the total number of disease sites and overall tumor volume was associated with overall survival. Those results suggest that TA may provide added value in the evaluation of patients with HGSOC, beyond the traditional evaluation of the sole peritoneal disease extent. They are in line with genetic data that have shown different mutational landscapes between primary ovarian lesions and peritoneal implants [60, 61]. Rizzo et al. evaluated whether CT radiomics features alone or combined with clinical data were associated with residual tumor at surgery in 101 patients with HGSOC and were able to predict the risk of disease progression within 12 months [84]. TA was performed on the primary ovarian tumor only. The authors found that radiomic features related to mass size, randomness and homogeneity were associated with residual tumor. Compactness1 below the median (in link with mass size), GrayLevelCooccurrenceMatrix25/0-1InformationMeasureCorr2 below the median (representing the degree of randomness within the mass) and GrayLevelCooccurrenceMatrix25/-333-1InverseVariance above the median (representing mass homogeneity) were associated with a higher risk of residual tumor after surgery [84]. The authors found as well that the risk of progression at 12 months was associated with three radiomic features. At multivariate analysis, F2 shape/ Max3DDiameter (in link with tumor size) was the single feature significantly associated with progression at 12 months. Adding this radiomic feature to a clinically based model significantly increased prediction of progression at 12 months by 14% (AUC = 0.73 for clinical model vs. 0.87 for clinical radiomic model) [84]. Based on these studies, it has been hypothesized that TA may serve as a new biomarker for patient selection for effective new therapies in the coming years, as well as anticipation of treatment resistant lesions (Figure 1).

How to perform TA?

To date, TA is not available for standard practice and usually requires in house developed software, although commercially available options are emerging. In this following chapter, we will briefly review the required steps to perform TA.

A post processing software is needed, either a commercially available tool or an in-house design, most of which are CT or MRI vendor neutral. As a post processing method, TA can be performed retrospectively and be briefly described in seven main steps below [85, 86].

Image acquisition

Image acquisition can be performed on the multiple modalities, e.g MRI, CT or PET scanner.

Image filtration

Images can be further filtered in order to reduce the noise, which an important issue with CT. Most of the heterogeneity on the CT images are due to photon noise, masking actual tissue heterogeneity [87]. The use of filters is therefore useful to reduce photon noise and improve tumor heterogeneity measurement [88]. These filters consist in methods of discretization that could be absolute or relative and the optimal number of level of grey for CT studies has been established by a recent consensus [89]. Of note, no consensus exists for MR imaging to date.

Image segmentation

For further analysis, tumor segmentation is a critical step. Region of interest (ROI) or volume of interest (VOI) are used to define the region in which features are calculated. This can be done manually, semi-automatically or automatically by dedicated software. Semi automatically methods are better than manually methods to optimize reproducibility of the different parameters extracted [90]The choice of the ROI or VOI is critical as it influences the quantification of the subsequent features [91]. Care to avoid contamination of the ROI/VOI by adjacent structures is mandatory.

Image interpolation:

TA requires interpolation to isotropic voxel spacing to be rotationally invariant, and to allow comparison between image data from different samples and cohorts. Voxel interpolation affects image feature values as many image features are sensitive to changes in voxel size. Maintaining consistent isotropic voxel spacing across different measurements and devices is therefore important for reproducibility. Different interpolation algorithms have been proposed to perform image interpolation[92].

Image re-segmentation

Image re-segmentation is an optional step that may be performed to remove voxels from the intensity mask that fall outside of a specified range. An example is the exclusion of voxels with Hounsfield units indicating air and bone tissue in the tumour ROI within CT images, or low activity areas on positron emission tomography/CT images.

Feature extraction

Various methods can be employed such as structural, model-based, statistical or frequency methods [93]. The statistical method is the most used for TA [85]. Radiomics features extracted by statistical methods during the sixth step, are divided into several order statistics that differ in the description of the gray level distribution in the image:

Shape parameters related to the description of 2D or 3D shape of the lesion.

First-order statistics (or intensity histogram) is related to the frequency distribution of the pixel intensity inside the ROI. The intensity-based statistical features describe how grey levels within the ROI are distributed. It includes common statistics what can be extracted from the histogram such as: mean, standard deviation, variance (measure the histogram width deviation around the mean), skewness (measure the asymmetry of the histogram around the mean). First-order histogram analysis does not account for the location of the pixels and lacks any reference to the spatial interrelationship between gray values (Figure 2).

Second-order statistics (or texture based features) characterize spatial relationships between pixels and are measured primarily from matrices such as co-occurrence matrices (e. g., gray level co-occurrence matrix [GLCM]) [92]. Those matrices evaluate the particular relationship between a pixel with a certain gray level with another pixel of another gray level, and this in the whole ROI and for all the pixels [85]. GLCM calculation is explained in Figure 3. Texture features computed from the GLCM consist of: energy (a measure of the amount of grey level variation within a given region), entropy (measurement of randomness or disorder in the distribution of signal intensities, variation), homogeneity (the uniformity in the distribution of co-occurrent intensity pairs), and contrast (a measure of variation in the distribution of co-occurrent intensity pairs).

Higher-order statistics examine location and relationships between three or more pixels and evaluate features such as contrast, coarseness, and busyness. Higher-order features have the advantage of evaluating voxels in their local context, taking the relationship with neighboring voxels into account.

Analysis

Finally, between 50 and 5000 features are extracted. This large number needs to be reduced by feature qualification to select only the features that are informative, reproducible on other similar studies and not redundant [92]. Many methods exist and may be classified into three categories: *i*), filtration methods for selecting parameters according to their strength and repeatability occurring during the different segmentation performed for example and according their non redundancy; *ii*) transformation methods for combining several parameters obtained in new ones including the analysis in main component or in descriptive component; *iii*) classification methods which may be supervised (probabilistic tree or support vector machine SVM for examples) or unsupervised (K-means clustering for example).

There are multiple methods of selection and classification. Indeed, Pamar et al. have studied 14 selection methods and 12 methods of classification applied on 440 parameters extracted from on a series of 464 CT examinations performed for lung cancers [94]. Complex multivariate statistical analysis was required to select the most accurate classification based on its AUC [92].

Challenges and limitations of TA

TA is still an emergent tool and its implementation in daily busy routine practice will requires optimization and standardization of each step [95]. For now, multiple platforms either commercially available or in-house applications have been used but their reproducibility need to be tested [91]. TA process from type of segmentation to the different features extracted vary widely across different platforms and studies, making the comparison and reproducibility of their results difficult [91]. Recently, an international panel of researchers have published a white paper regarding definitions and recommendations for methods used in radiomics studies [89].

Currently, no uniform measurement or reporting standards exist. Some authors have

proposed a practice standardization to establish which texture features are most helpful, general thresholds for what constitutes a heterogeneous lesion, and guidelines for imaging parameters for given texture features and thresholds to overcome this wide variability between studies [92].

Another major challenge is the huge amount of data produced by TA. The investigation of various features from a single dataset may increase the risk of type I error and as such lead to false results. A meta-analysis of multiple PET TA studies demonstrated that after applying a statistical correction, significant results were no longer found in many of the studies evaluated [96]. Use of statistical corrections, such as Holm-Bonferroni sequential correction, or validation datasets may be helpful for confirming the veracity of identified associations [96].

Finally, and particularly for ovarian cancer, large volume disease means time consuming manual segmentation. For now, automated software to segment the whole tumor burden are not available and as such disease areas need to be manually segmented which preclude routine evaluation. Manual segmentation requires delineation of tumor per slice; particularly time consuming in large and irregularly shaped tumors and challenging in case of infiltrative disease. A preliminary study, using an automated segmentation approach in rectal cancer has shown promising results [97]. Future work will focus on the development of complete automated post processing methods enabling the extraction of maximal information from the images with the added challenge to demonstrate a clinical benefit in the assessment of tumor response.

Conclusion

Subjective extraction of multiple qualitative parameters has shown a link between phenotypic CT features and gene pattern in ovarian cancer with the limitation of relatively poor interobserver agreement. Quantitative analysis using TA is challenging but has shown promising results regarding tumor heterogeneity on CT and patient outcome. Although many issues need to be addressed before implementation in clinical practice, TA will allow radiologists to obtain additional and more robust imaging data from studies that are already being performed and which could be combined with qualitative features. In the era of artificial intelligence these types of features could be incorporated into decision-support or computer-aided diagnosis tools to predict tumor aggressiveness and response to therapy.

Conflict of interest

The authors have no conflicts of interest to disclose

References

1. Gillies RJ, Kinahan PE, Hricak H. Radiomics: images are more than pictures, they are data. *Radiology* 2016 278:563-77.
2. Hillman RT, Chisholm GB, Lu KH, Futreal PA. Genomic rearrangement signatures and clinical outcomes in high-grade serous ovarian cancer. *J Natl Cancer Inst* 2018;110;doi: 10.1093/jnci/djx176.
3. Bruning A, Mylonas I. New emerging drugs targeting the genomic integrity and replication machinery in ovarian cancer. *Arch Gynecol Obstet* 2011;283:1087-96.
4. Hu T, Wang S, Huang L, Wang J, Shi D, Li Y, et al. A clinical-radiomics nomogram for the preoperative prediction of lung metastasis in colorectal cancer patients with indeterminate pulmonary nodules. *Eur Radiol* 2018;doi: 10.1007/s00330-018-5539-3.
5. Ortiz-Ramon R, Larroza A, Ruiz-Espana S, Arana E, Moratal D. Classifying brain metastases by their primary site of origin using a radiomics approach based on texture analysis: a feasibility study. *Eur Radiol* 2018;doi: 10.1007/s00330-018-5463-6.
6. She Y, Zhang L, Zhu H, Dai C, Xie D, Xie H, et al. The predictive value of CT-based radiomics in differentiating indolent from invasive lung adenocarcinoma in patients with pulmonary nodules. *Eur Radiol* 2018; doi: 10.1007/s00330-018-5509-9.
7. Tan X, Ma Z, Yan L, Ye W, Liu Z, Liang C. Radiomics nomogram outperforms size criteria in discriminating lymph node metastasis in resectable esophageal squamous cell carcinoma. *Eur Radiol* 2018;doi: 10.1007/s00330-018-5581-1.

8. Wang J, Wu CJ, Bao ML, Zhang J, Wang XN, Zhang YD. Machine learning-based analysis of MR radiomics can help to improve the diagnostic performance of PI-RADS v2 in clinically relevant prostate cancer. *Eur Radiol* 2017;27:4082-90.
9. Matzner-Lober E, Suehs CM, Dohan A, Molinari N. Thoughts on entering correlated imaging variables into a multivariable model: application to radiomics and texture analysis. *Diagn Interv Imaging* 2018;99:269-70.
10. Soyer P. Agreement and observer variability. *Diagn Interv Imaging* 2018;99:53-4.
11. Bonekamp D, Kohl S, Wiesenfarth M, Schelb P, Radtke JP, Gotz M, et al. Radiomic machine learning for characterization of prostate lesions with MRI: comparison to ADC values. *Radiology* 2018;289:128-37.
12. Kickingereeder P, Burth S, Wick A, Gotz M, Eidel O, Schlemmer HP, et al. Radiomic profiling of glioblastoma: identifying an imaging predictor of patient survival with improved performance over established clinical and radiologic risk models. *Radiology* 2016;280:880-9.
13. Kickingereeder P, Bonekamp D, Nowosielski M, Kratz A, Sill M, Burth S, et al. Radiogenomics of glioblastoma: machine learning-based classification of molecular characteristics by using multiparametric and multiregional MR imaging features. *Radiology* 2016;281:907-18.
14. Kuo MD, Jamshidi N. Behind the numbers: decoding molecular phenotypes with radiogenomics--guiding principles and technical considerations. *Radiology* 2014;270:320-5.
15. Pinker K, Chin J, Melsaether AN, Morris EA, Moy L. Precision medicine and radiogenomics in breast cancer: new approaches toward diagnosis and treatment. *Radiology* 2018;287:732-47.

16. Woodard GA, Ray KM, Joe BN, Price ER. Qualitative radiogenomics: association between oncotype DX test recurrence score and BI-RADS mammographic and breast MR imaging features. *Radiology* 2018;286:60-70.
17. Zhou M, Leung A, Echegaray S, Gentles A, Shrager JB, Jensen KC, et al. Non-small cell lung cancer radiogenomics map identifies relationships between molecular and imaging phenotypes with prognostic implications. *Radiology* 2018;286:307-15.
18. Karlo CA, Di Paolo PL, Chaim J, Hakimi AA, Ostrovnaya I, Russo P, et al. Radiogenomics of clear cell renal cell carcinoma: associations between CT imaging features and mutations. *Radiology* 2014;270:464-71.
19. Feng Z, Rong P, Cao P, Zhou Q, Zhu W, Yan Z, et al. Machine learning-based quantitative texture analysis of CT images of small renal masses: differentiation of angiomyolipoma without visible fat from renal cell carcinoma. *Eur Radiol* 2018;28:1625-33.
20. Giganti F, Antunes S, Salerno A, Ambrosi A, Marra P, Nicoletti R, et al. Gastric cancer: texture analysis from multidetector computed tomography as a potential preoperative prognostic biomarker. *Eur Radiol* 2017;27:1831-9.
21. Kim BR, Kim JH, Ahn SJ, Joo I, Choi SY, Park SJ, et al. CT prediction of resectability and prognosis in patients with pancreatic ductal adenocarcinoma after neoadjuvant treatment using image findings and texture analysis. *Eur Radiol* 2018; doi: 10.1007/s00330-018-5574-0.
22. Lakhman Y, Veeraraghavan H, Chaim J, Feier D, Goldman DA, Moskowitz CS, et al. Differentiation of uterine leiomyosarcoma from atypical leiomyoma: diagnostic accuracy of qualitative MR imaging features and feasibility of texture analysis. *Eur Radiol* 2017;27:2903-15.
23. Lisson CS, Lisson CG, Flosdorf K, Mayer-Steinacker R, Schultheiss M, von Baer A, et al. Diagnostic value of MRI-based 3D texture analysis for tissue characterisation and

discrimination of low-grade chondrosarcoma from enchondroma: a pilot study. *Eur Radiol* 2018;28:468-77.

24. Liu S, Liu S, Ji C, Zheng H, Pan X, Zhang Y, et al. Application of CT texture analysis in predicting histopathological characteristics of gastric cancers. *Eur Radiol* 2017;27:4951-9.

25. Shen Q, Shan Y, Hu Z, Chen W, Yang B, Han J, et al. Quantitative parameters of CT texture analysis as potential markers for early prediction of spontaneous intracranial hemorrhage enlargement. *Eur Radiol* 2018; doi: 10.1007/s00330-018-5364-8.

26. Wibmer A, Hricak H, Gondo T, Matsumoto K, Veeraraghavan H, Fehr D, et al. Haralick texture analysis of prostate MRI: utility for differentiating non-cancerous prostate from prostate cancer and differentiating prostate cancers with different Gleason scores. *Eur Radiol* 2015;25:2840-50.

27. Hodgdon T, McInnes MD, Schieda N, Flood TA, Lamb L, Thornhill RE. Can quantitative CT texture analysis be used to differentiate fat-poor renal angiomyolipoma from renal cell carcinoma on unenhanced CT images? *Radiology* 2015;276:787-96.

28. Imbriaco M, Cuocolo R. Does texture analysis of MR images of breast tumors help predict response to treatment? *Radiology* 2018;286:421-3.

29. Miles KA, Ganeshan B, Griffiths MR, Young RC, Chatwin CR. Colorectal cancer: texture analysis of portal phase hepatic CT images as a potential marker of survival. *Radiology* 2009;250:444-52.

30. Ng F, Ganeshan B, Kozarski R, Miles KA, Goh V. Assessment of primary colorectal cancer heterogeneity by using whole-tumor texture analysis: contrast-enhanced CT texture as a biomarker of 5-year survival. *Radiology* 2013;266:177-84.

31. Ueno Y, Forghani B, Forghani R, Dohan A, Zeng XZ, Chamming's F, et al. Endometrial carcinoma: MR imaging-based texture model for preoperative risk stratification-a preliminary analysis. *Radiology* 2017;284:748-57.
32. Kjaer L, Ring P, Thomsen C, Henriksen O. Texture analysis in quantitative MR imaging. Tissue characterisation of normal brain and intracranial tumours at 1.5 T. *Acta Radiol* 1995;36:127-35.
33. Skogen K, Schulz A, Helseth E, Ganeshan B, Dormagen JB, Server A. Texture analysis on diffusion tensor imaging: discriminating glioblastoma from single brain metastasis. *Acta Radiol* 2018; doi: 10.1177/0284185118780889.
34. Li Z, Mao Y, Li H, Yu G, Wan H, Li B. Differentiating brain metastases from different pathological types of lung cancers using texture analysis of T1 postcontrast MR. *Magn Reson Med* 2016;76:1410-9.
35. Haider MA, Vosough A, Khalvati F, Kiss A, Ganeshan B, Bjarnason GA. CT texture analysis: a potential tool for prediction of survival in patients with metastatic clear cell carcinoma treated with sunitinib. *Cancer Imaging* 2017;17:4.
36. Scrima AT, Lubner MG, Abel EJ, Havighurst TC, Shapiro DD, Huang W, et al. Texture analysis of small renal cell carcinomas at MDCT for predicting relevant histologic and protein biomarkers. *Abdom Radiol* 2018; doi: 10.1007/s00261-018-1649-2.
37. Horvat N, Veeraraghavan H, Khan M, Blazic I, Zheng J, Capanu M, et al. MR imaging of rectal cancer: radiomics analysis to assess treatment response after neoadjuvant therapy. *Radiology* 2018;287:833-43.

38. Ross JS, Ali SM, Wang K, Palmer G, Yelensky R, Lipson D, et al. Comprehensive genomic profiling of epithelial ovarian cancer by next generation sequencing-based diagnostic assay reveals new routes to targeted therapies. *Gynecol Oncol* 2013;130:554-9.
39. Wallbillich JJ, Forde B, Havrilesky LJ, Cohn DE. A personalized paradigm in the treatment of platinum-resistant ovarian cancer: a cost utility analysis of genomic-based versus cytotoxic therapy. *Gynecol Oncol* 2016;142:144-9.
40. Lee JY, Kim HS, Suh DH, Kim MK, Chung HH, Song YS. Ovarian cancer biomarker discovery based on genomic approaches. *J Cancer Prev* 2013;18:298-312.
41. Goringe KL, George J, Anglesio MS, Ramakrishna M, Etemadmoghadam D, Cowin P, et al. Copy number analysis identifies novel interactions between genomic loci in ovarian cancer. *PLoS One* 2010;5(9).
42. Mills AM, Peres LC, Meiss A, Ring KL, Modesitt SC, Abbott SE, et al. Targetable immune regulatory molecule expression in high-grade serous ovarian carcinomas in African-American women: a study of PD-L1 and IDO in 112 cases from the African-American Cancer Epidemiology Study (AACES). *Int J Gynecol Pathol* 2018;doi:10.1097/PGP.0000000000000494.
43. Siegel RL, Miller KD, Jemal A. Cancer statistics, 2018. *CA Cancer J Clin* 2018;68:7-30.
44. Torre LA, Trabert B, DeSantis CE, Miller KD, Samimi G, Runowicz CD, et al. Ovarian cancer statistics, 2018. *CA Cancer J Clin* 2018; doi: 10.3322/caac.21456.
45. Hennessy BT, Coleman RL, Markman M. Ovarian cancer. *Lancet* 2009;374:1371-82.
46. Herzog TJ. Recurrent ovarian cancer: how important is it to treat to disease progression? *Clin Cancer Res* 2004;10:7439-49.

47. Herzog TJ, Pothuri B. Ovarian cancer: a focus on management of recurrent disease. *Nat Clin Pract Oncol* 2006;3:604-11.
48. Konecny GE, Winterhoff B, Wang C. Gene-expression signatures in ovarian cancer: Promise and challenges for patient stratification. *Gynecol Oncol* 2016;141:379-385.
49. Patch AM, Christie EL, Etemadmoghadam D, Garsed DW, George J, Fereday S, Nones K, Cowin P, Alsop K, Bailey PJ et al. Whole-genome characterization of chemoresistant ovarian cancer. *Nature* 2015;521:489-94.
50. Cancer Genome Atlas Research N. Integrated genomic analyses of ovarian carcinoma. *Nature* 2011;474:609-15.
51. Petrillo M, Marchetti C, De Leo R, Musella A, Capoluongo E, Paris I, et al. BRCA mutational status, initial disease presentation, and clinical outcome in high-grade serous advanced ovarian cancer: a multicenter study. *Am J Obstet Gynecol* 2017;217:334 e331-9.
52. Skubitz AP, Pambuccian SE, Argenta PA, Skubitz KM. Differential gene expression identifies subgroups of ovarian carcinoma. *Transl Res* 2006;148:223-48.
53. Stanescu AD, Ples L, Edu A, Olaru GO, Comanescu AC, Poteca AG, et a. Different patterns of heterogeneity in ovarian carcinoma. *Rom J Morphol Embryol* 2015;56:1357-63.
54. Nymoer DA, Hetland-Falkenthal TE, Holth A, Ow GS, Ivshina AV, Trope CG, et al. Expression and clinical role of chemoresponse-associated genes in ovarian serous carcinoma. *Gynecol Oncol* 2015;139:30-9.
55. Zangwill BC, Balsara G, Dunton C, Varello M, Rebane BA, Hernandez E, Atkinson BF. Ovarian carcinoma heterogeneity as demonstrated by DNA ploidy. *Cancer* 1993;71:2261-7.

56. Mota A, Trivino JC, Rojo-Sebastian A, Martinez-Ramirez A, Chiva L, Gonzalez-Martin A, et al. Intra-tumor heterogeneity in TP53 null high grade serous ovarian carcinoma progression. *BMC Cancer* 2015;15:940.
57. Bashashati A, Ha G, Tone A, Ding J, Prentice LM, Roth A, et al. Distinct evolutionary trajectories of primary high-grade serous ovarian cancers revealed through spatial mutational profiling. *J Pathol* 2013;231:21-34.
58. De Mattos-Arruda L, Weigelt B, Cortes J, Won HH, Ng CK, Nuciforo P, et al. Capturing intra-tumor genetic heterogeneity by de novo mutation profiling of circulating cell-free tumor DNA: a proof-of-principle. *Ann Oncol* 2014;25:1729-35.
59. Sala E, Kataoka MY, Priest AN, Gill AB, McLean MA, Joubert I, et al. Advanced ovarian cancer: multiparametric MR imaging demonstrates response- and metastasis-specific effects. *Radiology* 2012;263:149-59.
60. Tothill RW, Tinker AV, George J, Brown R, Fox SB, Lade S, et al. Novel molecular subtypes of serous and endometrioid ovarian cancer linked to clinical outcome. *Clin Cancer Res* 2008;14:5198-208.
61. Verhaak RG, Tamayo P, Yang JY, Hubbard D, Zhang H, Creighton CJ, et al. Prognostically relevant gene signatures of high-grade serous ovarian carcinoma. *J Clin Invest* 2013;123:517-25.
62. Vargas HA, Wassberg C, Fox JJ, Wibmer A, Goldman DA, Kuk D, et al. Response. *Radiology* 2015;274:625.
63. Vargas HA, Huang EP, Lakhman Y, Ippolito JE, Bhosale P, Mellnick V, et al. Radiogenomics of high-grade serous ovarian cancer: multireader multi-institutional study from the cancer genome atlas ovarian cancer imaging research group. *Radiology* 2017;285:482-92.

64. Oktay K, Turan V, Titus S, Stobezki R, Liu L. BRCA mutations, DNA repair deficiency, and ovarian aging. *Biol Reprod* 2015;93:67.
65. Tutt A, Ashworth A. The relationship between the roles of BRCA genes in DNA repair and cancer predisposition. *Trends Mol Med* 2002;8:571-6.
66. Farmer H, McCabe N, Lord CJ, Tutt AN, Johnson DA, Richardson TB, et al. Targeting the DNA repair defect in BRCA mutant cells as a therapeutic strategy. *Nature* 2005;434:917-21.
67. Turner N, Tutt A, Ashworth A. Targeting the DNA repair defect of BRCA tumours. *Curr Opin Pharmacol* 2005;5:388-93.
68. Johannsson OT, Ranstam J, Borg A, Olsson H: Survival of BRCA1 breast and ovarian cancer patients: a population-based study from southern Sweden. *J Clin Oncol* 1998;16:397-404.
69. Boyd J, Sonoda Y, Federici MG, Bogomolny F, Rhei E, Maresco DL, et al. Clinicopathologic features of BRCA-linked and sporadic ovarian cancer. *JAMA* 2000;283:2260-5.
70. Risch HA, McLaughlin JR, Cole DE, Rosen B, Bradley L, Kwan E, et al. Prevalence and penetrance of germline BRCA1 and BRCA2 mutations in a population series of 649 women with ovarian cancer. *Am J Hum Genet* 2001;68:700-10.
71. Chetrit A, Hirsh-Yechezkel G, Ben-David Y, Lubin F, Friedman E, Sadetzki S. Effect of BRCA1/2 mutations on long-term survival of patients with invasive ovarian cancer: the national Israeli study of ovarian cancer. *J Clin Oncology* 2008;26:20-5.
72. Veltman J, Mann R, Kok T, Obdeijn IM, Hoogerbrugge N, Blickman JG, et al. Breast tumor characteristics of BRCA1 and BRCA2 gene mutation carriers on MRI. *Eur Radiol* 2008;18:931-8.

73. Artioli G, Borgato L, Cappetta A, Wabersich J, Mocellin S, Dalla Palma M, et al. Overall survival in BRCA-associated ovarian cancer: case-control study of an Italian series. *Eur J Gynecol Oncol* 2010; 31:658-61.
74. Gallagher DJ, Konner JA, Bell-McGuinn KM, Bhatia J, Sabbatini P, Aghajanian CA, et al. Survival in epithelial ovarian cancer: a multivariate analysis incorporating BRCA mutation status and platinum sensitivity. *Ann Oncol* 2011;22:1127-32.
75. Yang D, Khan S, Sun Y, Hess K, Shmulevich I, Sood AK, et al. Association of BRCA1 and BRCA2 mutations with survival, chemotherapy sensitivity, and gene mutator phenotype in patients with ovarian cancer. *JAMA* 2011; 306:1557-65.
76. Hyman DM, Zhou Q, Iasonos A, Grisham RN, Arnold AG, Phillips MF, et al. Improved survival for BRCA2-associated serous ovarian cancer compared with both BRCA-negative and BRCA1-associated serous ovarian cancer. *Cancer* 2012; 118:3703-9.
77. Liu J, Cristea MC, Frankel P, Neuhausen SL, Steele L, Engelstaedter V, et al. Clinical characteristics and outcomes of BRCA-associated ovarian cancer: genotype and survival. *Cancer Genet* 2012; 205:34-41.
78. Lorusso D, Cirillo F, Mancini M, Spatti GB, Grijuela B, Ditto A, et al. The different impact of BRCA mutations on the survival of epithelial ovarian cancer patients: a retrospective single-center experience. *Oncology* 2013;85:122-7.
79. Nougaret S, Lakhman Y, Gonen M, Goldman DA, Micco M, D'Anastasi M, et al. High-grade serous ovarian cancer: associations between BRCA mutation status, CT imaging phenotypes, and clinical outcomes. *Radiology* 2017;285:472-81.

80. Kaas R, Kroger R, Peterse JL, Hart AA, Muller SH. The correlation of mammographic and histologic patterns of breast cancers in BRCA1 gene mutation carriers, compared to age-matched sporadic controls. *Eur Radiol* 2006;16:2842-8.
81. Reyes MC, Arnold AG, Kauff ND, Levine DA, Soslow RA. Invasion patterns of metastatic high-grade serous carcinoma of ovary or fallopian tube associated with BRCA deficiency. *Modern Pathol* 2014; 27:1405-11.
82. Soslow RA, Han G, Park KJ, Garg K, Olvera N, Spriggs DR, et al. Morphologic patterns associated with BRCA1 and BRCA2 genotype in ovarian carcinoma. *Modern Pathol* 2012; 25:625-36.
83. Vargas HA, Veeraraghavan H, Micco M, Nougaret S, Lakhman Y, Meier AA, et al. A novel representation of inter-site tumour heterogeneity from pre-treatment computed tomography textures classifies ovarian cancers by clinical outcome. *Eur Radiol* 2017; 27:3991-4001.
84. Rizzo S, Botta F, Raimondi S, Origgi D, Buscarino V, Colarieti A, et al. Radiomics of high-grade serous ovarian cancer: association between quantitative CT features, residual tumour and disease progression within 12 months. *Eur Radiol* 2018; 28:4849-59.
85. Davnall F, Yip CS, Ljungqvist G, Selmi M, Ng F, Sanghera B, et al. Assessment of tumor heterogeneity: an emerging imaging tool for clinical practice? *Insights Imaging* 2012;3:573-89.
86. Ganeshan B, Miles KA: Quantifying tumour heterogeneity with CT. *Cancer Imaging* 2013;13:140-9.
87. Markel D, Naqa IE, Freeman C, Vallieres M. SU-E-J-110: A novel level set active contour algorithm for multimodality joint segmentation/registration using the Jensen-Renyi divergence. *Med Phys* 2012;39:3678.

88. Hatt M, Majdoub M, Vallieres M, Tixier F, Le Rest CC, Groheux D, et al. 18F-FDG PET uptake characterization through texture analysis: investigating the complementary nature of heterogeneity and functional tumor volume in a multi-cancer site patient cohort. *J Nucl Med* 2015;56:38-44.
89. Zwanenburg A, Leger S, Vallières M, Löck S. Initiative for the IBS. Image biomarker standardisation initiative. <http://arxiv.org/abs/161207003> 2018.
90. Parmar C, Rios Velazquez E, Leijenaar R, Jermoumi M, Carvalho S, Mak RH, et al. Robust radiomics feature quantification using semiautomatic volumetric segmentation. *PLoS One* 2014;9:e102107.
91. Zhao B, Tan Y, Tsai WY, Qi J, Xie C, Lu L, Schwartz LH. Reproducibility of radiomics for deciphering tumor phenotype with imaging. *Sci Rep* 2016;6:23428.
92. Vallieres M, Zwanenburg A, Badic B, Cheze Le Rest C, Visvikis D, Hatt M. Responsible radiomics research for faster clinical translation. *J Nucl Med* 2018, 59:189-93.
93. Lubner MG, Smith AD, Sandrasegaran K, Sahani DV, Pickhardt PJ. CT texture analysis: definitions, applications, biologic correlates, and challenges. *Radiographics* 2017;37:1483-503.
94. Parmar C, Grossmann P, Bussink J, Lambin P, Aerts HJ. Machine learning methods for quantitative radiomic biomarkers. *Sci Rep* 2015;5:13087.
95. Berenguer R, Pastor-Juan MDR, Canales-Vazquez J, Castro-Garcia M, Villas MV, Mansilla Legorburo F, Sabater S: Radiomics of ct features may be nonreproducible and redundant: influence of ct acquisition parameters. *Radiology* 2018;288:407-15.
96. Galavis PE, Hollensen C, Jallow N, Paliwal B, Jeraj R. Variability of textural features in FDG PET images due to different acquisition modes and reconstruction parameters. *Acta Oncol* 2010;49:1012-6.

97. van Heeswijk MM, Lambregts DM, van Griethuysen JJ, Oei S, Rao SX, de Graaff CA, et al. Automated and semiautomated segmentation of rectal tumor volumes on diffusion-weighted MRI: can it replace manual volumetry? *Int J Radiat Oncol Biol Phys* 2016;94:824-31.

FIGURE LEGENDS

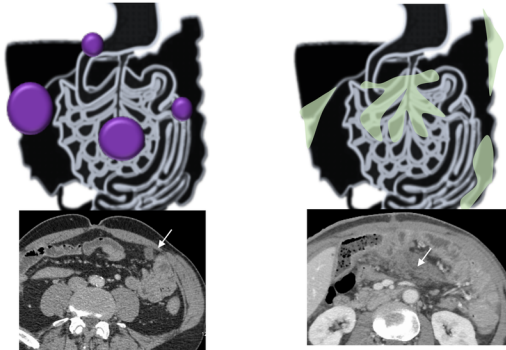
Figure 1. Drawing summarizing advances in research in ovarian cancer radiomics.

Figure 2. First-order statistical-based CT texture parameters. Plot of the pixel histogram, where the x-axis represents gray-level values and the y-axis represents the frequency of occurrence. First-order parameters include the mean of the histogram (vertical red line), standard deviation and 95 of the histogram (horizontal blue line). When the distribution has a larger tail to the left, the skew is negative (and the skew is positive when the tail is larger to the right). The term kurtosis designates how pointy or smooth the curve is compared to a normal distribution (right). Kurtosis describes the peakedness of the pixel histogram. A pointier or more peaked histogram is seen with positive and progressively higher kurtosis values (right).

Figure 3. Second-order statistical-based texture parameters. (a) and (b) show diagrams of two different gray-scale images. Each of the square contains the same number of different shade-of-grey “pixels,” so the first-order texture features and pixel histograms are nearly identical for these two images. However, second-order texture features that take into account pixel location and relationship to adjacent pixels, such as gray-level co-occurrence matrix are different between these two images. The grey- scales of the image can be represented by discrete values (c). The gray-level co-occurrence matrix measures the frequency with which each type of pixel occurs in the horizontal, vertical, and oblique planes adjacent to all other pixels (d). The number of co-occurrences of pixel pairs for a given search window are counted and a grey level co-occurrence matrix is established.

**Subjective Radiomics Analysis:
Qualitative DATA**

Phenotypic association between CT features and Gene alterations



BRCA +

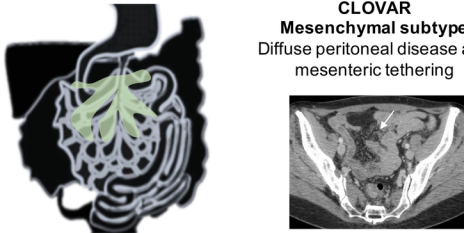
Nodular pattern and lower risk of mesenteric involvement

BRCA -

Infiltrative pattern and higher risk of mesenteric involvement

Nougaret et al, Radiology 2017

**CLOVAR
Mesenchymal subtype**
Diffuse peritoneal disease and mesenteric tethering

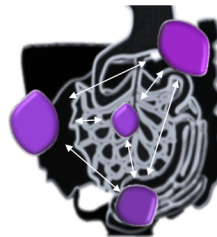


Vargas et al, Radiology 2015

**Objective Radiomics Analysis:
Quantitative DATA with Texture analysis**

Inter-Site (Spatial) Tumour Texture Heterogeneity May Predict Outcome Irrespective of CLOVAR Gene Signature

Inter-tumoral Heterogeneity evaluation using texture analysis and an inter-site similarity matrix



Patient with fewer inter-site dissimilarities have a better outcome regardless their CLOVAR gene signature



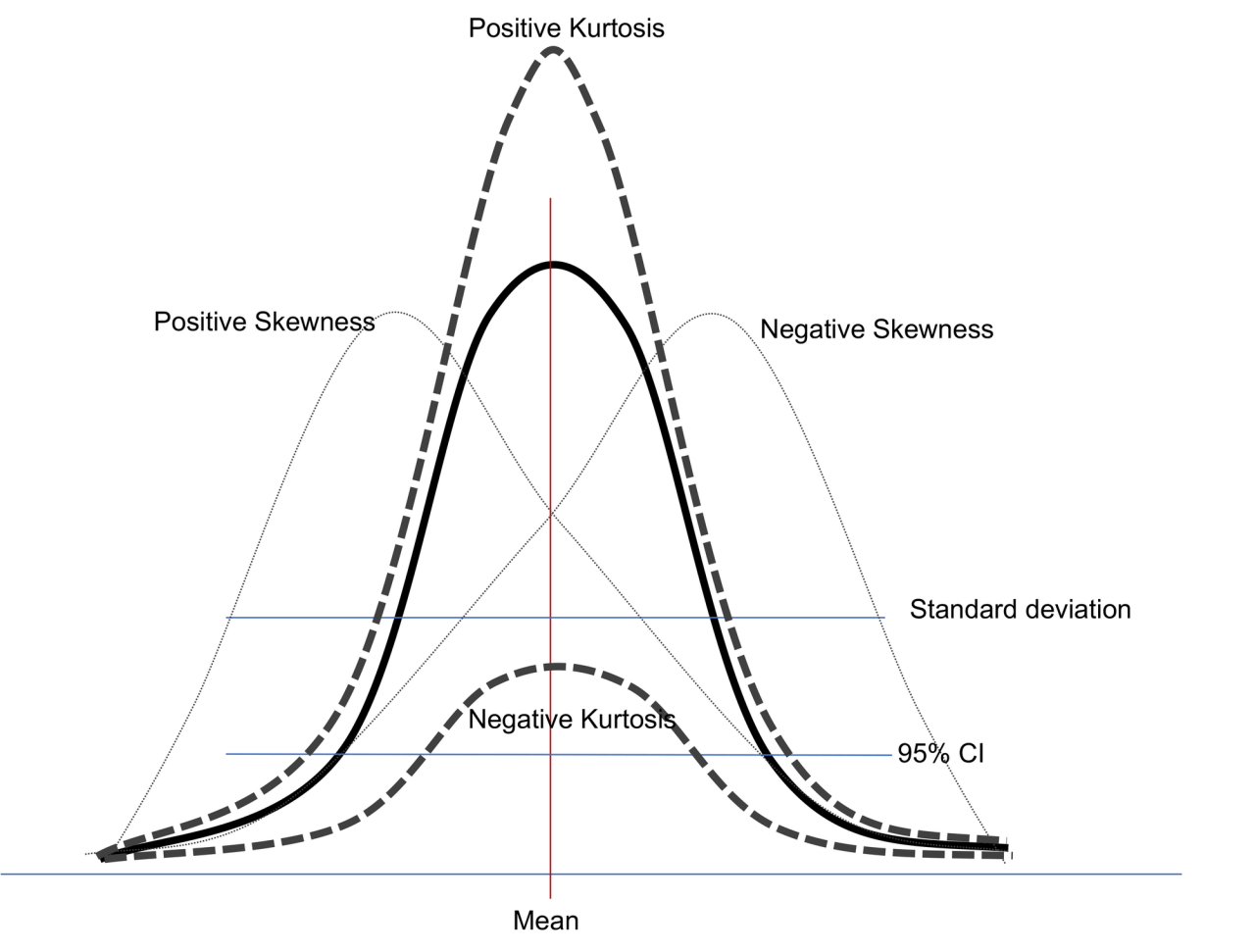
Patient with higher inter-site dissimilarities have a poorer outcome regardless their CLOVAR gene signature

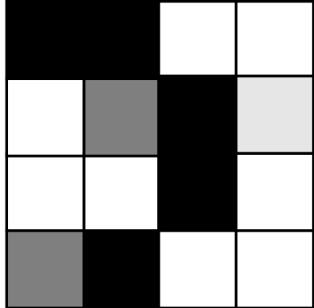
Vargas et al, European Radiology 2017



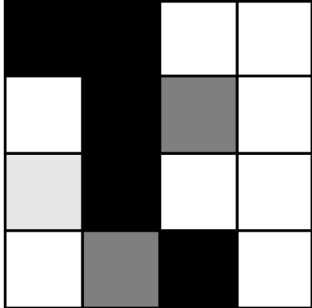
- Radiomic features related to ovarian mass size, randomness and homogeneity were associated with residual tumor at surgery
- A model including clinical and radiomic features performed better than only-clinical model to predict progression of the disease at 12 months

Rizzo et al, European Radiology 2018





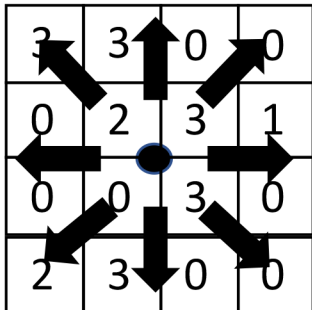
a



b

3	3	0	0
0	2	3	1
0	0	3	0
2	3	0	0

c



d